OPTICAL EMISSION SPECTROSCOPY OF CADMIUM DOMINATED DISCHARGES APPLIED FOR ASSESSMENT OF EXPLOSION PROTECTION

R. Methling[a,*], St. Franke[a], C. Uber[b], B. Barbu[c], F. Berger[c], M. Hilbert[b], D. Uhrlandt[a]

[a] *Leibniz Institute for Plasma Science and Technology (INP), Felix-Hausdorff-Str. 2, 17489 Greifswald, Germany*

[b] *Physikalisch-Technische Bundesanstalt (PTB), Bundesallee 100, 38116 Braunschweig, Germany*

[c] *Technische Universität Ilmenau, Gustav-Kirchhoff-Str. 1, PF 100565, 98684 Ilmenau, Germany*

[*] methling@inp-greifswald.de

Abstract. An assessment for the safe use of electrical equipment in explosive atmospheres can be performed with the aid of a spark test apparatus. Therefore, an anodic tungsten wire with 200 μm diameter is moved along the surface of a rotating cadmium disc (cathode). The explosion chamber enclosing the electrodes is filled with a highly explosive mixture of hydrogen and air. Depending on surface topology and relative movement of the contact pair, discharges occur randomly. A model contact device is used to investigate the plasma properties and the discharge characteristics near the thermo-chemical ignition threshold of the explosive atmosphere that typically occur at voltages around 30 V and currents around 30 mA. Spectroscopic investigations reveal that the emission of the discharges is dominated by atomic lines of cadmium, which allow the determination of distribution temperatures.

Keywords: optical emission spectroscopy, cadmium, explosion protection.

1. Introduction

All electrical equipment to be operated in explosive atmospheres needs to be assessed with respect to explosion protection issues. Therefore, a special spark test apparatus have been developed according to an international standard [1]. In this apparatus more or less defined electrical discharges are generated in an explosive atmosphere, simulating contact discharges occurring in electrical equipment. Since the results scatter and are poorly reproducible, alternatives to the spark test apparatus should be developed. Therefore, the physical mechanisms of such contact break discharges have to be analyzed and a multi-physical model is to be developed.

In explosion protection, the ignition behavior of explosive atmospheres by electric discharges has been extensively investigated, if they are initiated by high voltages [2–5]. These papers focus only on the electrical discharge or the thermodynamic relationships of the ignition for high-voltage discharges with fixed electrode spacings. However, electrical discharges can also occur at low voltages during contact opening and contact closing. Those discharges have so far only been partially investigated [2, 6–8]. For a modeling of discharges by contact processes that are able to initiate thermo-chemical reaction of an explosive gas mixture, these investigations are not sufficient. Recently, electrical discharges occurring during contact opening have been characterized by Uber [7]. Typically, they are operated near the minimum ignition energy (17 μJ for H_2/air mixture with 21 % H_2 volume fraction) and occur at voltages below 30 V and currents above

30 mA. The emission spectra of these discharges are found to be dominated by atomic lines from metal vapor [9, 10]. However, the investigation of spatio-temporal evolution of basic plasma parameters is still lacking, which should form the basis for further modeling and evaluation criteria for the thermo-chemical ignition or non-ignition of a discharge.

In this contribution we present spectroscopic investigations of contact break discharges operated between a cadmium cathode and a tungsten anode in ambient atmosphere. Conclusions are drawn on the plasma temperature and the local thermal equilibrium (LTE).

2. Experimental

The experimental setup is presented in figure 1. A contact device was placed in an explosion chamber with quartz windows. The experiments presented here were performed in ambient air instead of hydrogen-air mixture. The tip of a tungsten wire of about 200 μm diameter was placed in contact with a cadmium block. The Cd block was moved along the tip with a speed of ≈0.002 m/s. Occasionally, the W wire was lifted up from the Cd surface in order to interrupt the direct contact and thus, to initialize a horizontally drawn discharge. This upward movement had an average speed in the range of 0.1 m/s.

The contact device was powered by a low-current DC source with a constant current of 60 mA at a maximum voltage of 30 V (for details see [7]). The W wire was operated as anode and the Cd block as cathode. The discharge had an initial voltage of about 10 V that can be attributed to the electrode sheaths.
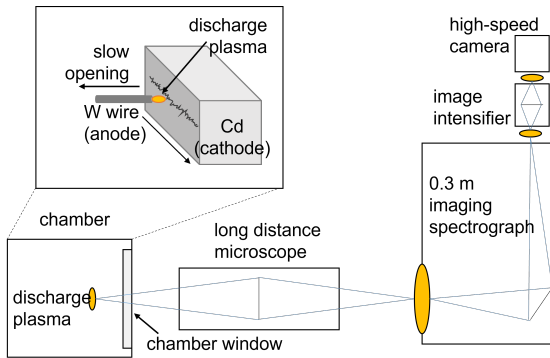
Figure 1. Experimental setup: The discharge is ignited between the W wire and the Cd block that are moved along each other. A long distance microscope is used to image the magnified discharge onto the widely opened entrance slit of the spectrometer equipped with intensifier and high-speed camera.

Figure 2. Example of an two-dimensional spectroscopic image (848 x 300 pixels). The vertical structures represent multiple images of the discharge at different wavelengths (horizontal dimension) limited by W anode at the top and Cd cathode at the bottom.

It extended up to 200 μm before the limit of 30 V was reached and the discharge was interrupted. Hence, the electric field strength was in the range of 100 V/mm.

Optical emission spectroscopy (OES) was performed with a 0.3 m-imaging spectrometer using a grating of 300 lines/mm (Acton Research). The discharge was imaged by means of a far-field microscope (QM1, Questar) with its axial dimension parallel to the slit jaws of the spectrograph. The entrance slit was widely open (3 mm). With a magnification around a factor 10, the full discharge had a maximum axial dimension of around 200 μm and an approximate radial dimension of 100 μm. A high-speed camera (Fastcam SA5, Photron) boosted with an image intensifier (C10880, Hamamatsu) was mounted to the spectrometer. Thus, a spatial resolution lower than 10 μm was achieved (pixel resolution 2.3 μm/px). The spectroscopic images were taken at a frame rate of 10,000 fps ($\approx$ 100 μs exposure time) as a compromise between radiation intensity and temporal resolution. The electrical characteristics were recorded with an oscilloscope (DL9040L, Yokogawa) and appropriate probes. Relative spectral intensity calibration was carried out using a tungsten strip lamp (OSRAM Wi 17/G).

3. Results and Discussion

The OES recording covers 848×300 pixels and displays multiple images of the discharge at different wavelengths. An example frame is shown in figure 2. It was acquired about 2 ms after contact separation and immediately before discharge quenching. The two-dimensional frame is rather complex. As usual for imaging spectroscopy, the vertical axis gives the spatial resolution along the electrode gap, showing a discharge length of about 162 μm. The horizontal axis, however, can provide more information than just an usual 1D spectrum due to the large entrance slit, i.e. spectral and spatial information is combined. Assuming monochromatic light emission, e.g. from an atomic line at a single wavelength, a full image of
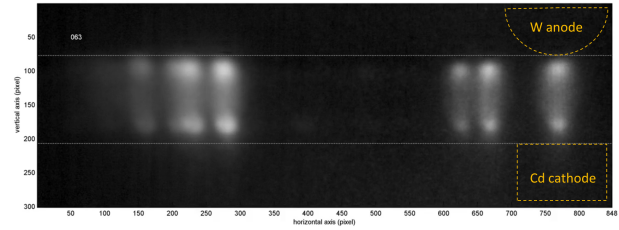
the discharge is spectrally diffracted at the grating and imaged onto the focal plane of the spectrograph. Regarding a spectrum consisting of several widely separated lines, a number of such discharge images will be visible as it can be seen for most of the lines in figure 2. Nevertheless, if the spectral separation between the lines is not sufficient, an overlap will occur, cf. the second discharge image from the left. To summarize, the images originating from different lines can only be resolved if the spectral distance is large enough compared with the (in our case huge) apparatus profile. More details about this 2D OES technique can be found e.g. in [11].

The single images of the discharge at different wavelengths are partially overlapping. From measurements with smaller apparatus profile it is known that the broadening of the spectral lines was much less than the width of the features visible in the OES image. At the right side of figure 2 the contour of the tungsten wire and the location of the cadmium surface were sketched schematically. As the tungsten wire was approximately 200 μm in diameter and the magnification was a factor of 10; the open slit width was slightly larger than the diameter of the tungsten wire.

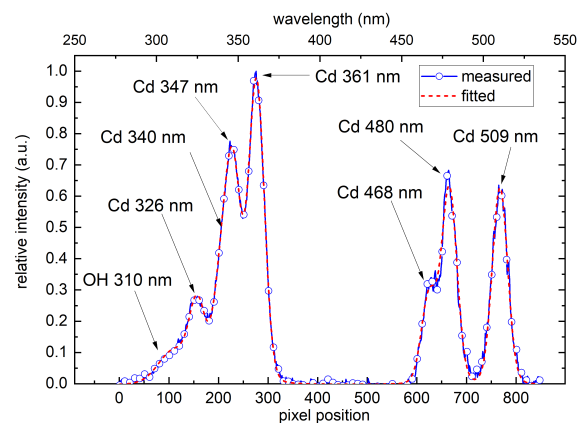Figure 3 shows the intensity distribution in the

Figure 3. Blue curve (circles): Intensity distribution (spectrum) in middle of the electrode gap. Red: Emission intensity fitted by Gauss functions.
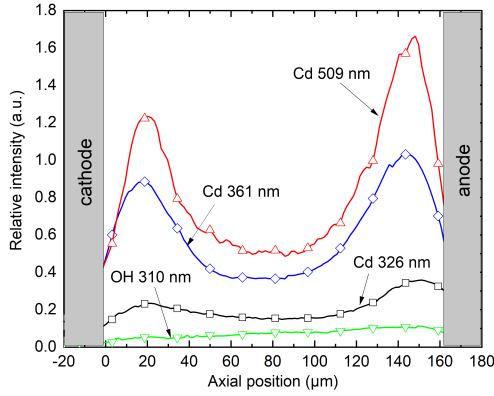
Figure 4. Axial intensity distribution of selected spectral lines.

λ (nm)	A_{ul} (1/s)	E_l (eV)	g_l	E_u (eV)	g_u
326.105	4.06E+05	0.00000	1	3.80087	3
340.365	7.70E+07	3.73366	1	7.37529	3
346.620	1.60E+08	3.80087	3	7.37679	5
361.051	1.55E+08	3.94604	5	7.37904	7
467.815	1.30E+07	3.73366	1	6.38320	3
479.991	4.10E+07	3.80087	3	6.38320	3
508.582	5.60E+07	3.94604	5	6.38320	3

Table 1. Atomic data for selected Cd lines observed from discharge retrieved from NIST database.

horizontal stripe in the middle between the electrodes (blue curve with circles). For further evaluation, this radial profile was fitted by several Gauss functions with 25 to 35 pixels FWHM after taking account of the instrumental profile of the spectrometer. The spectral features in figure 3 could be identified as atomic spectral lines of cadmium and the molecular band of OH at 310 nm. No atomic lines from the gases (N, O) or other bands from molecules (N$_2$, O$_2$, NO) were observed in the applied wavelength range or in according overview measurements.

As a result of the fit routine, the axial evolution of peak intensity at different wavelengths for selected spectral lines is presented in figure 4. Obviously, all Cd lines show more or less pronounced emission peaks in front of both cathode and anode. From the line ratios it should be possible to determine plasma temperatures. For simplification, two neighboring lines around Cd 347 nm and two others around Cd 361 nm have been incorporated into effective transition probabilities, as they originate from similar upper energy levels [12]. The summarized emission coefficient ϵ of two neighboring lines a and b is given by:

$$\epsilon^a + \epsilon^b \sim \left(A_{ul}^a + \frac{A_{ul}^b g_u^b}{g_u^a} \right) \quad (1)$$

Here, A is the transition probability and g is the statistical weight of the upper and lower level. The term in brackets is the effective transition probability. Atomic data have been retrieved from NIST lines database. An overview on the atomic data utilized for temperature evaluation is given in table 1.

As it can be seen from table 1, Cd lines in the investigated wavelength range originate from three different upper energy levels which form three groups of spectral lines. Hence, the plasma temperature from Boltzmann plot can be calculated for different combinations of spectral lines.

The level distribution temperature shown in figure 5 was deduced from the slope of a straight line between
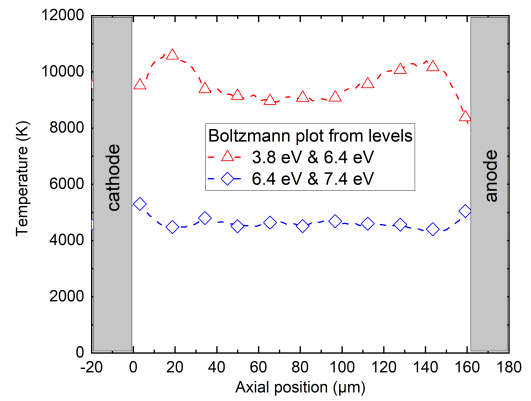

Figure 5. Axial distribution of plasma temperatures from Boltzmann fits using different energy levels.

two points in the Boltzmann plot. The red curve with triangles was obtained for 3.80 eV and 6.38 eV, which provided plasma temperatures around 10,000 K. The lower temperature of around 5,000 K was obtained from a Boltzmann plot using the points at 6.38 eV and 7.38 eV (blue diamonds). The errors in temperatures resulting from experiment (measurement accuracy, intensity calibration, uncertainties of transition values) were estimated to be relatively low, probably below 1000 K. Obviously, temperatures obtained for different level pairs are not the same and local thermodynamic equilibrium cannot be assumed. This is a novel finding based on experimental evidence. Previous investigation found indications for deviations from LTE by comparison of experimental results with numerical calculations [9, 10].

Another finding was the observation of OH molecular emission, which has not been considered before and obviously originates from ambient air humidity. It could be proven that intensity was sufficient for diagnostic evaluation. OH is an important marker for thermo-chemical reactions in explosive atmospheres containing oxygen and hydrogen, and hence will be helpful in future investigation of discharges in H$_2$-air mixtures.
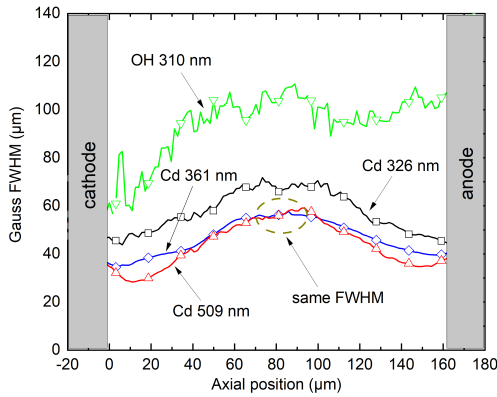
Additional to axial temperature distribution, also

Figure 6. Axial distribution of radial intensity profile width fitted by Gauss full width at half maximum (FWHM).
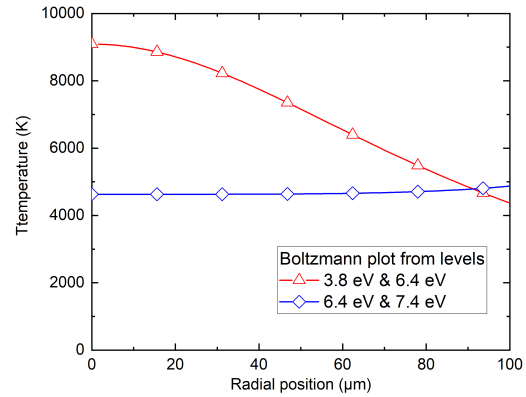

Figure 7. Radial temperature distributions in the middle between the electrodes according to Gauss full width at half maximum (FWHM) for different combinations of atomic lines.

information on the radial profiles can be extracted from the 2D OES images. Figure 6 shows the widths fitted to the profiles as presented in figure 3 for each axial position between the electrodes. It can be seen that for the group of lines around Cd 361 nm and the line Cd 509 nm the width and therefore the radial decay of intensity is similar in the middle between the electrodes. The width relates to how flat or steep a cross section is at a certain position. If the FWHM is the same for two lines, then the ratio between the lines will be constant for all (radial) positions. As a consequence, the equal widths of radial intensity profiles lead to a radially constant temperature in the middle between the electrodes as shown in the blue curve in figure 7 (within the experimental uncertainties). However, the radial temperature profiles obtained from the other combination of energy levels show a clear decay of distribution temperature (cf. red curve in figure 7). That means energy levels at $6.38\,\mathrm{eV}$ and $7.38\,\mathrm{eV}$ are much faster depopulated towards outer radial positions than the energy level at $3.8\,\mathrm{eV}$. This is another proof for non-LTE in the discharges investigated here, as for plasma in LTE the radial course of temperature must decay towards ambient air temperature for thermodynamic considerations. A radially constant distribution temperature moreover indicates a radially constant electric field which determines the excitation cross section in collisional-radiative plasmas.

4. Conclusions

It was shown that the contact break discharges between Cd and W electrodes as utilized in explosion protection are not in LTE. This finding is obtained from experimental results making use of optical emission spectroscopy. Future investigations including the design of theoretical model will have to take account of this feature.

References

[1] International Electrotechnical Commission. *IEC 60079-11, Explosive atmospheres. Part 11: Equipment protection by intrinsic safety.* IEC, Geneve, Switzerland, 2011.

[2] V. Babrauskas. *Ignition handbook.* Fire Science Publishers, Issaquah (WA), USA, 2003. ISBN 978-0-9728111-3-2.

[3] R. Eckhoff and W. Olsen. A new method for generation of synchronized capacitive sparks of low energy. *J. Electristatics*, 68:73–78, 2010.

[4] S. Essmann. *Experimentelle Untersuchung der Zündung durch elektrostatische Entladungen geringer Energie.* PhD thesis, Karlsruher Institut für Technologie (KIT), 2019. ISBN 978-3-95606-445-6. doi:10.7795/110.20190709.

[5] M. Hattwig and H. Steen, editors. *Handbook of Explosion Prevention and Protection.* Wiley VCH, Weinheim, 2008. ISBN 9783527612475.

[6] U. Johannsmeyer. *Zündung explosionsfähiger Gemische durch kurzzeitige Schliessfunken in kapazitiven Stromkreisen für die Zündschutzart Eigensicherheit.* PhD thesis, TU Braunschweig, 1984.

[7] C. Uber. *Charakterisierung elektrischer Kontakt-Entladungen im Bereich niedriger Spannungen im Zündgrenz-Bereich von Wasserstoff-Luft-Gemisch.* PhD thesis, TU Ilmenau, 2019. www.db-thueringen.de/receive/dbt_mods_00039103.

[8] Z. Zborovszky and L. Cotugno. *Evaluation of the Cadmium Disc Breakflash in testing Electrical Circuits. A Comprehensive Study of Intrinsic Safety Criteria.* Bureau of Mines Open File Report. Denver Research Institute, University of Denver, 1974.

[9] C. Uber, T. Runge, J. Brunzendorf, et al. Electrical discharges caused by opening contacts in an ignitable atmosphere. Part II: Spectroscopic investigation and estimation of temperatures. *J. Loss Prevention in the Process Industries*, 61:213–219, 2019. `doi:10.1016/j.jlp.2019.05.010`.

[10] R. Shekhar, S. Gortschakow, H. Grosshans, et al. Numerical investigation of transient, low-power metal vapour discharges occurring in near limit ignitions of flammable gas. *J. Phys. D Appl. Phys.*, 52(4):045202, 2019. `doi:10.1088/1361-6463/aaed04`.

[11] J. W. Olesik and G. M. Hieftje. Optical imaging spectrometers. *Anal. Chem.*, 57(11):2049–2055, 1985. `doi:10.1021/ac00288a010`.

[12] W. Lochte-Holtgreven. *Evaluation of Plasma Parameters*. American Institute of Physics, New York, 1995. ISBN 9781563963889.